ESD-TR-86-234

MTR-9750

PREDICTING ANTENNA SIDELOBE PERFORMANCE

By

PHILIP D. KAPLAN

AUGUST 1986

Prepared for

DEPUTY COMMANDER FOR STRATEGIC SYSTEMS
ELECTRONIC SYSTEMS DIVISION
AIR FORCE SYSTEMS COMMAND
UNITED STATES AIR FORCE
Hanscom Air Force Base, Massachusetts

Approved for public release; distribution unlimited.

Project No. 5150

Prepared by

THE MITRE CORPORATION
Bedford, Massachusetts

Contract No. F19628-84-C-0001

ADA172708

REVIEW AND APPROVAL

This technical report has been reviewed and is approved for publication.

Jeremiah Q. Hamilton

JEREMIAH Q. HAMILTON, GS-12
Project Engineer

William N. Keto

WILLIAM N. KETO, GM-13
Director, Advanced
Programs and Integration

FOR THE COMMANDER

GARRY W. CURL, COLONEL, USAF
Director, Management Services
Deputy Commander for Strategic Systems

UNCLASSIFIED

SECURITY CLASSIFICATION OF THIS PAGE

REPORT DOCUMENTATION PAGE

1a. REPORT SECURITY CLASSIFICATION Unclassified	1b. RESTRICTIVE MARKINGS
2a. SECURITY CLASSIFICATION AUTHORITY	3. DISTRIBUTION/AVAILABILITY OF REPORT Approved for public release, distribution unlimited.
2b. DECLASSIFICATION/DOWNGRADING SCHEDULE	
4. PERFORMING ORGANIZATION REPORT NUMBER(S) MTR-9750 ESD-TR-86-234	5. MONITORING ORGANIZATION REPORT NUMBER(S)
6a. NAME OF PERFORMING ORGANIZATION The MITRE Corporation	6b. OFFICE SYMBOL (If applicable)
7a. NAME OF MONITORING ORGANIZATION	
6c. ADDRESS (City, State and ZIP Code) Burlington Road Bedford, MA 01730	7b. ADDRESS (City, State and ZIP Code)
8a. NAME OF FUNDING/SPONSORING ORGANIZATION Deputy Commander for (cont.)	8b. OFFICE SYMBOL (If applicable) ESD/SCU-1
9. PROCUREMENT INSTRUMENT IDENTIFICATION NUMBER F19628-84-C-0001	
8c. ADDRESS (City, State and ZIP Code) Electronic Systems Division, AFSC Hanscom AFB, MA 01731-5000	10. SOURCE OF FUNDING NOS.

PROGRAM ELEMENT NO.	PROJECT NO.	TASK NO.	WORK UNIT NO.
	5150		

11. TITLE (Include Security Classification)
PREDICTING ANTENNA SIDELOBE PERFORMANCE

12. PERSONAL AUTHOR(S)
Kaplan, Philip D.

13a. TYPE OF REPORT	13b. TIME COVERED	14. DATE OF REPORT (Yr., Mo., Day)	15. PAGE COUNT
Final	FROM ______ TO ______	1986 August	41

16. SUPPLEMENTARY NOTATION

17. COSATI CODES		
FIELD	GROUP	SUB. GR.

18. SUBJECT TERMS (Continue on reverse if necessary and identify by block number)
Antenna Sidelobe Performance
Array Tolerances
Phased Arrays
Planar Arrays
Tolerances/Overdesign

19. ABSTRACT (Continue on reverse if necessary and identify by block number)

Given a set of antenna array performance requirements, the dimensions and illumination taper of an ideal array may be determined. However, random errors in actual manufacturing lead to uncertainty as to actual array performance. It is shown here that the performance is nonetheless predictable with a probability function that rests on the contractor's decisions in the fabrication of the array. The derivation of curves that relate this probability function to a range of conditions, overdesign allowances and production tolerances, is the salient feature of this paper.

When sidelobe specifications allow for occasional statistical "pop-ups," the specified levels may be better adapted to requirements. The contractor, it turn, could decide on the proper choice between overdesign and tolerances, in a measured response to the specified performance.

20. DISTRIBUTION/AVAILABILITY OF ABSTRACT UNCLASSIFIED/UNLIMITED ☒ SAME AS RPT. ☐ DTIC USERS ☐	21. ABSTRACT SECURITY CLASSIFICATION Unclassified

22a. NAME OF RESPONSIBLE INDIVIDUAL	22b. TELEPHONE NUMBER (Include Area Code)	22c. OFFICE SYMBOL
Diana F. Arimento	(617)271-7454	Mail Stop D230

DD FORM 1473, 83 APR EDITION OF 1 JAN 73 IS OBSOLETE.

UNCLASSIFIED

SECURITY CLASSIFICATION OF THIS PAGE

8a. Strategic Systems.

ACKNOWLEDGMENTS

The application of analysis that was first performed on the radar detection process to the problems of predicting antenna sidelobe performance is better appreciated by the reader having some familiarity in the two disparate fields. In reviewing this paper, I was fortunate in having included Roger E. Clapp and F. N. Eddy, both having expertise in antennas and radar detection. Their review stimulated discussions and their suggestions were gratefully included in the paper.

In addition to editorial comments, I am indebted to Roger for improvements in the clarity of description. Figure 2 in this report has been added at his suggestion and provides the reader with a pictorial concept of sidelobe parameters.

To Neal I owe the elaboration in the concept of antenna gain. Antenna gain is germane to sidelobes (whether they be design, residual or measured), since sidelobes are referred to antenna gain. Following the delineation of gain given in reference 6, this paper explicitly refers to "antenna gain factor" or "directive gain" in their appropriate places. This gain distinction would nevertheless allow one to change gain references, when the change is appropriately adjusted for the element gain factor.

This document has been prepared by The MITRE Corporation under Project No. 5150, Contract No. F19628-84-C-0001. The contract is sponsored by the Electronic Systems Division, Air Force Systems Command, Hanscom Air Force Base, Massachusetts 01731.

TABLE OF CONTENTS

LIST OF ILLUSTRATIONS

LIST OF TABLES

SECTION 1

INTRODUCTION

Planar array performance, as ultimately demonstrated by antenna patterns, is most simply characterized in its principal planes. Patterns are shaped in each principal plane to separate and independent requirements. Given a set of requirements, the dimensions and illumination taper for the array may be determined. However, as a result of production error tolerances, the designer would still be uncertain of the actual array performances. It is shown here that the performance is nonetheless predictable in a statistical sense, using a probability function that is associated with the design and fabrication of the rows and columns of the array. The derivation of curves that relate this probability function to a range of conditions, overdesign allowance and production tolerances, is the salient feature of this paper.

In practice, perfectly accurate amplitude and phase control on individual array elements can not be realized. These errors in general degrade the sidelobes from their design levels. (Although changes in the mainlobe gain and pointing angle would also result from the errors, this paper deals with sidelobe degradation only.) Random circuit errors tend to add an average "noise" power to the theoretically designed peak sidelobe levels [1]. The relationship of noise power to element errors is derived in appendix A and plotted in figure 1.

Sidelobes in all space are seen to be composed of two components: a design level that is mathematically described and a residue that is random. Sidelobe predictions are analogous to the predictions of signal-plus-noise, as first analyzed by Rice [2]. The Rician probability function serves as a mathematical basis for target detection, enabling the user to predict threshold crossings with computed probabilities, such as target detections or false alarms. The probability of a signal plus noise exceeding a specified threshold is analogous to the likelihood of a sidelobe exceeding a specified level. In this analogy, correspondence holds between signal and sidelobe design value, noise and a random residue, threshold and specified peak sidelobe. The Rician function computational process is given in appendix B, and related curves are plotted in figures 3 and 4.

Peak sidelobe statistical predictability provides a more meaningful measure for assessing vulnerability to sidelobe interference. Since the peak and not the average sidelobes degrade performance, the probability associated with peaks is a better indicator.

The peak probability function better serves the user in formulating sidelobe specifications and the manufacturer in meeting the specifications. The user, mindful of the statistical behavior, can moderate the specifications to allow for a number of random "pop-ups" and, as a consequence, to better adapt the specifications to the vulnerability requirements. The contractor, in turn, can decide on the proper choice between overdesign and tolerances in a measured response to the specified performance. The contractor's decision is taken from a wide range of choices: from a design that is close to specifications and that keeps tight tolerances, to an

alternative design that has substantially lower sidelobes and that relaxes the tolerances. For the same probability, the decision is dictated by the relative risks and costs of enlarging the array as compared with the risks and costs of maintaining tight tolerances. The ultimate decision would rest on the contractor's judgment.

SECTION 2

AVERAGE SIDELOBE RESIDUE

2.1 SIDELOBE RESIDUE EQUATION

The average residue power in the sidelobes, caused by production errors in the fabrication of element circuits, is assumed to be uniform in all angle space. These errors would be random and characterized by a standard deviation in amplitude and phase. The average residue power, normalized to the array gain factor, has been derived in appendix A and repeated below.

$$S_{res}^{2} = \frac{\rho^2 + \phi^2}{g_A} \tag{1}$$

S_{res}^{2}	=	average residue power normalized to the array gain factor
ρ	=	rms amplitude ratio error (error/design amplitude)
ϕ	=	rms phase error in radians
g_A	=	array gain factor for row or column of the array

In figure 1, plots are derived from equation (1) for average residue power vs. rms errors for several parametric values of gain. The curves were computed separately for amplitude and phase errors and their respective powers added to yield the net residue. They illustrate the relationship of residual power, gain, and error tolerances.

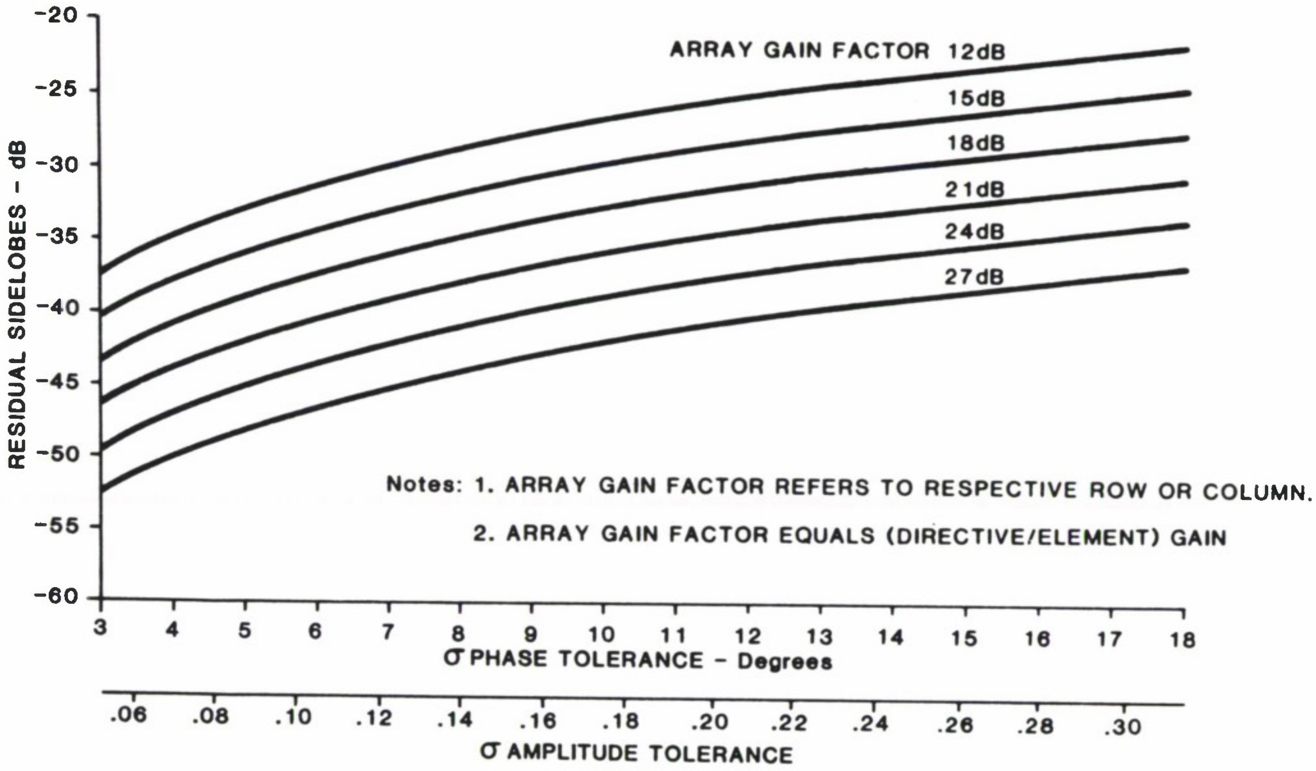

Figure 1. Residual Sidelobe Function of Manufacturing Tolerances

2.2 CONCEPTUAL EQUIVALENCE TO NOISE MODULATION

It is instructive to note the conceptual equivalence of sidelobe power as given in equation (1) and sideband power generated from a noise-like, flat modulation band. Let the power density in the modulation band be denoted m^2 and the incremental power in the frequency interval Δf within the band as $m^2 \Delta f$. For the case of small signal modulation, a pair of corresponding sidebands is produced that share the modulation power, each sideband being equal to m^2 $(\Delta f/2)$ (carrier amplitude assumed to be unity). The same sideband power relationship holds for either form of modulation, amplitude, or phase. That is, if we designate the modulation power $\rho^2 \Delta f$ as associated with amplitude modulation (AM) and $\phi^2 \Delta f$ as associated with phase modulation (PM), then the sideband power expressed for both forms in the general case is

$$\text{incremental sideband power} = \frac{\rho^2 + \phi^2}{2} \Delta f \tag{2}$$

ρ^2 : power density of modulation band associated with AM
ϕ^2 : power density of modulation band associated with PM
Δf : effective noise bandwidth in incremental modulation power
$\rho\sqrt{\Delta f}, \phi\sqrt{\Delta f}$: rms modulation index or degree of modulation

A comparison of equations (1) and (2) leads to the relationship

$$\Delta f = 2/g_A = \Delta\theta \tag{3}$$

By analogy with Δf, $\Delta\theta$ in the right-hand side of equation (3) may be interpreted as the "effective integration angle" of sidelobe residue power. The effective angle accordingly defines the interval

of taking independent samples of residue in angle space. Samples of residue less than $\Delta\theta$ would be partially correlated.

The relation of effective angle to the 3 dB beamwidth may be obtained by substituting for g_A in (3) the equivalent beamwidth (bw) as derived in appendix A, equation (A.14). This results in

$$\Delta\theta = 2\ (\mathrm{bw})\ (s/\lambda)/0.886 \qquad (4)$$

where s/λ is the element spacing in wavelengths. For example, for half wavelength spacing, $\Delta\theta$ from (4) equates to 1.13 (bw) signifying that the two are approximately equal.

2.3 ON ESTIMATING SIDELOBE RESIDUE POWER

A hypothetical example is taken of a manufacturing process of an array involving a series of acceptance tests. At each test point acceptance limits are set for amplitude and phase. Production units that measure within limits are unchanged, otherwise they are replaced with acceptable units. Deviations from design values are assumed to be uniform within the set limits. The processing flow and tabulated data are given in table 1.

$$\begin{array}{c}k^{th}\\ \text{element}\\ \text{radiator}\end{array} \longrightarrow \begin{array}{c}\text{element}\\ \text{feed}\end{array} \xrightarrow{1} \begin{array}{c}\text{element}\\ \text{receiver}\end{array} \xrightarrow{2} \text{beamformer} \xrightarrow{3} \begin{array}{c}\text{mth}\\ \text{beam}\end{array}$$

Table 1

Example in Manufacturing Process Tolerances

Test Point	Acceptance Limits		rms	
	amp, dB	phase	ρ	ϕ
1	$\pm$ 0.25	$\pm 2^{o}$	0.0166	.02
2	$\pm$ 0.5	$\pm 3^{o}$	0.033	.03
3	$\pm$ 1.0	$\pm 5.5^{o}$	0.0665	.0554
		net	0.076	0.066

The acceptance limits in dB divided by 8.686 equate to the fractional error acceptance limits, and further division by $\sqrt{3}$ yields the rms fractional error. Thus $\pm$ 0.25 dB amplitude acceptance limits are equivalent to $\pm$ 0.0288 fractional error limits and yield an rms value for ρ of 0.0166. Also, the acceptance limits in phase divided by $\sqrt{3}$ yield the rms phase error, which is listed in radians. The net values were computed from the square root of the sum of the squares in the respective columns.

From equation 1, the residual sidelobes are computed for the net errors derived above, and for an assumed directive gain of the array of 21 dB.

$$S_R{}^2 = \frac{(.076)^2 + (.066)^2}{126} = 80.4 \times 10^{-6} = -41 \text{ dB} \tag{5}$$

The residual sidelobes may also be determined from figure 1. From the 21 dB gain curve, one reads minus 44.5 dB at 3.8° phase tolerance (.066 radians) and minus 43 dB at .076 amplitude tolerance. The sum of these power contributions is

$$\text{net residue} = 10 \log (10^{-4.45} + 10^{-4.3}) = -40.7 \text{ dB}$$

It is apparent that when the amplitude and phase errors are equal the net residue is obtained by adding 3 dB to the readings of either of the error curves.

SECTION 3

PREDICTABILITY OF SIDELOBE PEAKS

3.1 PROBABILITY CURVES

Sidelobe variability is modeled for a combination of design and random component values. The design component is mathematically described in all space and the values are "unfluctuating." The random component is assumed Gaussian, having a uniform variance (average power) in angle space when taken in correlation intervals of approximately the three dB beamwidth (see equation 4). The predictability problem is modeled identically to signal (non-fluctuating) and noise, analyzed by Rice, and follows Rician probability curves of the form given in equation (6). The computational process associated with equation (6) as used in this report is given in appendix B.

$$p(E/R) = (E/R^2)\left[\exp -(E^2 + P^2)/2R^2\right] \; I_o \; (EP/R^2) \qquad (6)$$

E = ensemble of design plus random variable
R = rms random component
P = peak design component
I_o = Bessel function of zero order, imaginary argument

In the case of sidelobes, there are three parameters of interest: the specified, design and residual values (see figure 2). The specified is dictated by the user's requirements and sets a bound for sidelobe peaks. The design or theoretical values combine randomly with the residue component into a composite sidelobe

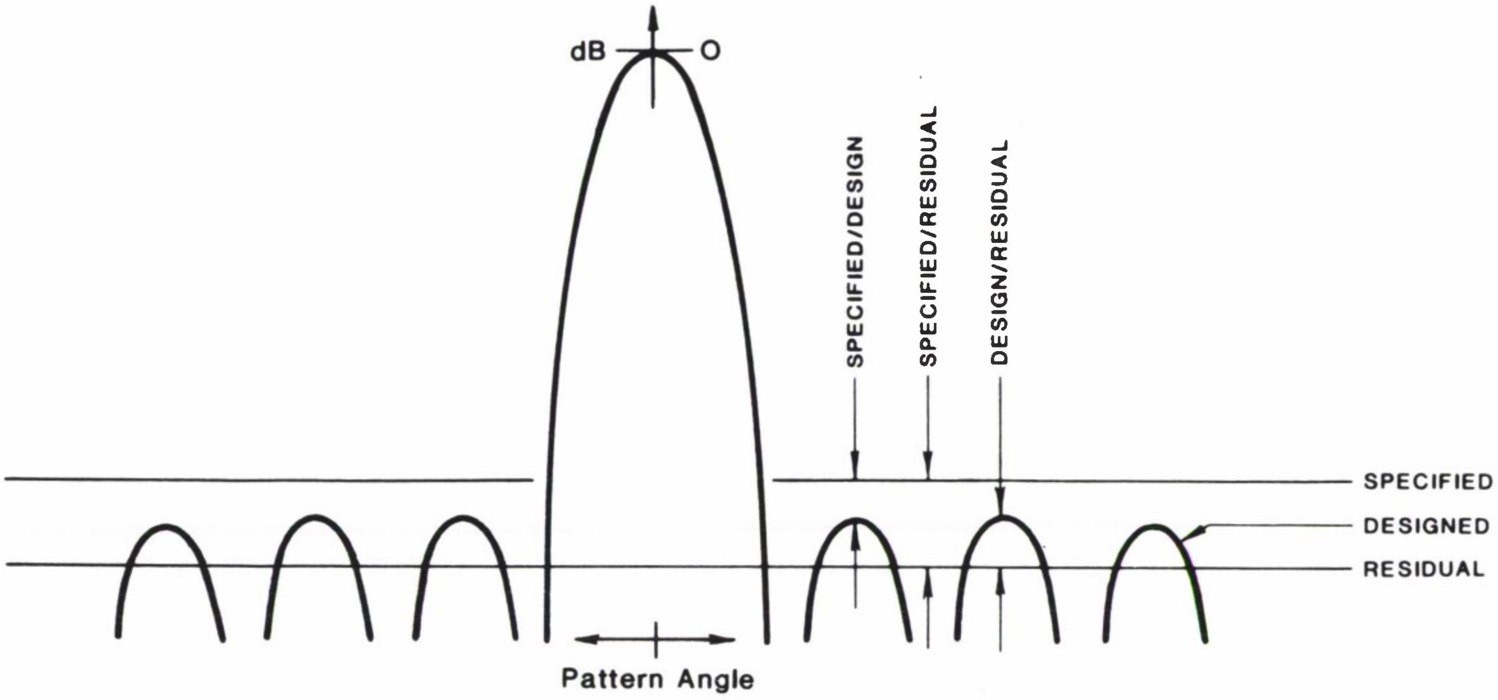

Figure 2. Sidelobe Pattern Parameters

variable. Various combinations of the three parameters yield corresponding probabilities: the probability that the composite sidelobe does not exceed the specification.

In figure 3, the parameters relate to the residual component; the probability is plotted against varying specifications for parametric values of design ratios. In figure 4, the parameters relate to the specified level; the curves illustrate the sensitivities of the design and residual ratios for given probabilities.

In these plots, it becomes apparent that there are trade-offs between the residual and design components in achieving a given probability. For example, taking the case of 0.9 probability, figure 4 covers the range of trade-offs for ratio pairs (residual, design) from (15 dB, 2.5 dB) to (8 dB, 11 dB). In choosing the former pair, a relatively tight tolerance is maintained that allows for an "overdesign" of only 2.5 dB. In choosing the latter pair, the tolerance is relaxed (in the equivalence of 7 dB) but calls for an overdesign of 11 dB (a change of 8.5 dB).

An optimum choice in minimizing costs and risks would primarily depend on estimations of their respective sensitivities to both overdesign and change in tolerance. The choice would be independently exercised for various array configurations, the radiating elements, and feed distributions, as well as for differences in row and column designs. The curves in figures 3 and 4, however, offer the contractor a guide to making the desirable choice.

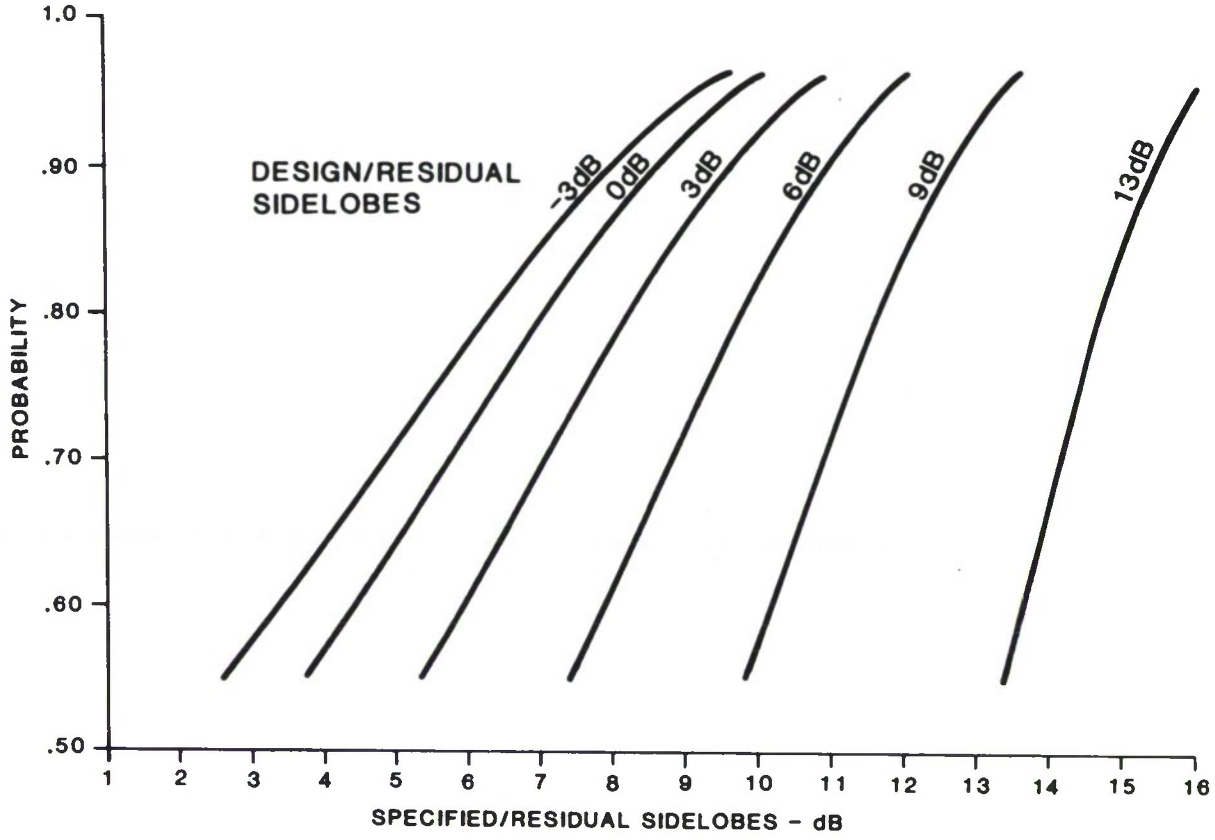

Figure 3. Probability Function Not to Exceed Specified Sidelobes

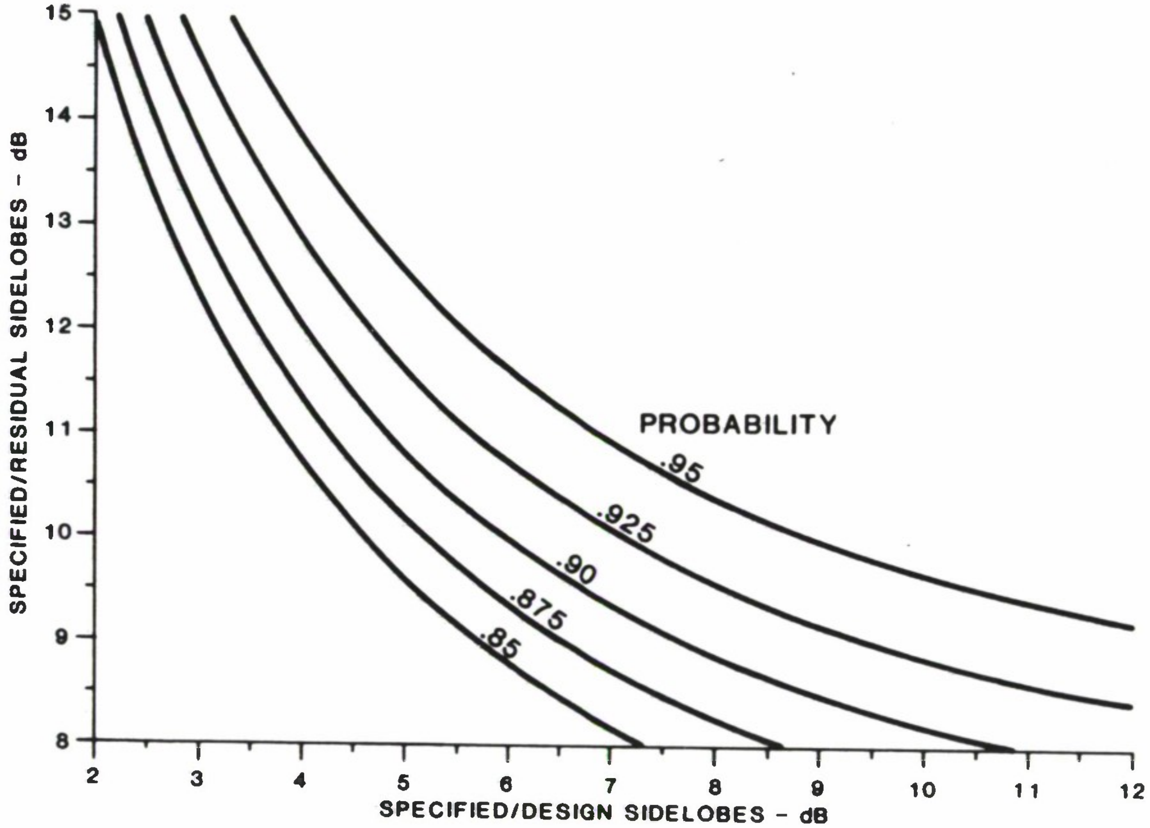

Figure 4. Residual and Design Trade-off for a Given Probability

In figure 4 it is interesting to note the region on the probability curves having a minus one slope. In the minus one slope region, dBs in design changes trade for equal dBs in residual changes. For the case when cost and risk sensitivities are comparable, the coordinate pairs in the minus one region would be optimum. As seen from figure 4, this region allows for a wide range of choices.

3.2 ON SIDELOBE SPECIFICATIONS

Sidelobe performance is more effectively specified when sidelobes are moderated to allow for statistical "pop-ups." Sidelobe levels can then be better responsive to the requirements. By analogy, the probability of detection p, referred to in radar detection specifications, allows for a number of statistical "misses" equal to 1 - p. The specified target size and range then respond better to mission requirements than had detection specifications not allowed any misses. In the latter case, the contractor's "actual" choice of probability of detection would be irrelevant.

Near broadside, the angle interval of cyclic recurrence of design peaks, approximately the 3 dB beamwidth, is also the approximate interval of independent residue samples (see equation 4). Therefore each such interval offers an independent possibility of exceeding the specified threshold, with a probability that varies with the design peak and residue components.

Assume the use of an efficient illumination function, as with a Taylor taper that has equal sidelobe peaks in the near-in region. As the residue power is equally distributed, the probability of not

exceeding the specified threshold in that region stays the same. Let P_0 denote the probability and let N be the number of independent intervals in that region, then from the binomial distribution we get

$$\text{prob (pop-ups} \leq k) = \sum_{n=o}^{k} C_n^N P_0^{\ N-n} (1-P_0)^n \qquad (7)$$

where

$$C_n^N = N!/n!(N-n)!$$

is the combination of N things taken n at a time. For example, when N equals 10 and P_0 equals 0.9, equation (7) assumes the following tabulated values

Table 2

Example of Probability of Pop-ups

k	prob (pop-ups < k)
0	.349
1	.736
2	.93
3	.987

Beyond the near-in sidelobe region, the performance may be expected to be as good or better than the near-in region, primarily due to progressively smaller peak values.

In order to ensure the user against the occurrence of severe pop-ups due to grating lobes, a cap on pop-up extremes may be specified. The cap level need only relax by 3 to 6 dB with respect to the pop-up specification level and the probability of exceeding

the cap level becomes exceeding small. One may therefore specify the cap level as "never" to be exceeded with reasonable confidence for success.

SECTION 4

SUMMARY

Statistical predictions of sidelobe performance have been derived on the basis of the Rician probability function as it relates to three pattern parameters: the specified, design and residual. Probability curves have been generated for a wide range of parametric ratios as the probability that the composite of design and residual components of the sidelobe does not exceed the specification.

The design component is mathematically described in all angle space and its value is unfluctuating. The residual adds a random component to the sidelobes, assumed to be Gaussian and having a uniform variance in angle space.

The residual component is caused by random production errors in the fabrication of element circuits, characterized by a standard deviation in amplitude and phase. Correlated production errors are not included in this analysis as such errors are conceivably possible to compensate in some systematic manner. The average residue power as a function of random production errors is given in equation (A.7) as normalized to the array gain factor.

The array gain factor as given in equation (A.8) is computed from the taper sequence function. The taper sequence, involving the amplitude distribution and number of elements, determines the design sidelobe peak values. For both the design and residual sidelobe components the basic normalization factor is therefore associated

with the array gain factor. The element gain is basically irrelevant in the analysis of either the design or residual sidelobes.

However, in antenna gain and pattern measurements, the operative gain is the directive gain, i.e., the gain resulting from the product of array and element gain factors. Furthermore, sidelobe specifications are implicitly made with reference to directive gain and verified from pattern measurements. When the design and residue components of sidelobes are observed in pattern measurements, the element gain must be factored in the readings as given in equation (A.11).

The probability function curves may serve the user in formulating more effective specifications that better respond to the user's requirements. The curves also offer guidelines to the contractor in the trade-off between overdesign and tolerance limits. When the cost/risks sensitivities are considered against incremental changes in design and tolerance limits, an optimum choice may be derived for a wide choice of performance objectives.

LIST OF REFERENCES

1. Skolnik, M. I., Introduction to Radar Systems, Second Edition, New York: McGraw-Hill, 1980, p. 139.

2. Rice, S. O., "Mathematical Analysis of Random Noise" in Wax, N., Selected Papers on Noise and Stochastic Processes, New York: Dover Publications, 1954.

3. North, D. O., "An Analysis of the Factors Which Determine Signal/Noise Discriminations in Pulsed Carrier Systems," Proceedings of the IEEE, July 1963, pp. 1016-1027.

4. Hsiao, J. K., "Array Sidelobes, Error Tolerance, Gain, and Beamwidth," NRL Report 8841, Naval Research Laboratory, Washington, DC, 28 September 1984.

5. Reference Data for Radio Engineers, Sixth Edition, New York: ITT (Howard W. Sams & Co.), 1977

6. Skolnik, M. I., Radar Handbook, New York: McGraw-Hill, 1970, pp. 11-23.

APPENDIX A

DERIVATION OF SIDELOBE RESIDUE NORMALIZED TO ARRAY GAIN FACTOR

A.1 ANALYSIS OF PATTERN RESIDUE

The normalized pattern equation of a linear array of N elements having a taper function sequence $\{A_n\}$ is

$$S = \sum_{n=1}^{N} A_n \exp(in\psi) / \sum_{n=1}^{N} A_n \qquad (A.1)$$

A_n = design amplitude of the nth element
ψ = $2\pi(s/\lambda)(\sin\theta - \sin\theta_p)$
s/λ = element spacing in wavelength
θ_p = beam pointing angle
θ = pattern angle

With element errors in amplitude and phase, the perturbed pattern may be expressed

$$S' = \sum a_n A_n \exp(in\psi + i\phi_n) \Big/ \sum A_n \qquad (A.2)$$

$a_n A_n$ = actual amplitude of the nth element having error factor a_n
ϕ_n = phase error of the nth element

The residue pattern, defined as the difference between the ideal and perturbed patterns, becomes

$$S_{res} = S' - S = \sum (a_n e^{i\phi_n} - 1) A_n \exp(in\psi) \Big/ \sum A_n \qquad (A.3)$$

The residue power pattern, the product of S_{res} and its complex conjugate, when averaged over many patterns becomes

$$\overline{S_{res}{}^{2}} = \overline{S_{res} \times S^{*}_{res}} \tag{A.4}$$

$$= \frac{\overline{\sum A_n [(a_n \cos\phi_n - 1) + i a_n \sin\phi_n] * \sum A_m [(a_m \cos\phi_m - 1) - i a_n \sin\phi_m]}}{(\sum A_n)^2}$$

In equation (A.4), we let $\psi = 0$ without loss of generality, since the mean residue is independent of pattern angle. In order to reduce the expression in (A.4) the following assumptions are made:

The errors are unbiased, i.e., $\overline{a}_\kappa = 1$ and $\overline{\phi}_\kappa = 0$. Consequently, terms in (A.4) involving $(a_\kappa \cos\phi_\kappa - 1)$ and $\sin\phi_\kappa$ are as likely to be positive as negative and will be independent for each κ. From the above assumptions, terms in the expansion of (A.4) equate to the following:

$$\overline{(a_n \cos\phi_n - 1)(a_m \cos\phi_m - 1)} = \begin{cases} \overline{(a_n \cos\phi_n - 1)^2}, & m = n \\ 0, & m \neq n \end{cases}$$

$$\overline{a_n \sin\phi_n \; a_m \sin\phi_m} = \begin{cases} \overline{a_n^2 \sin\phi_n^2} & m = n \\ 0, & m \neq n \end{cases}$$

$$\overline{(a_n \cos\phi_n - 1) \, a_m \sin\phi_m} = 0$$

The expansion of (A.4) may now be reduced as

$$\overline{\left|S_{res}\right|^2} = \overline{\Sigma A_n^2 \, [(a_n \cos\phi_n - 1)^2 + a_n^2 \sin^2\phi_n]} \Big/ (\Sigma A_n)^2 \qquad \text{(A.5)}$$

Since the average of the sum equals the sum of the average, the numerator in the right-hand side of (A.5) equates to

$$\Sigma A_n^2 \, \overline{[(a_n \cos\phi_n - 1)^2 + a_n^2 \sin^2\phi_n]}$$

Factoring the A_ns out of the average process, since the set of A_ns is design coefficients and invariant in the averages, we get

$$\Sigma A_n^2 \, \overline{[(a_n \cos\phi_n - 1)^2 + a_n^2 \sin^2\phi_n]} = \overline{[(a\cos\phi - 1)^2 + a^2 \sin^2\phi]} \, \Sigma A_n^2$$

The dropping of the subscript n in the right-hand side of the equation above is consistent with having equal averages for all n. The bracketed terms are therefore factored out of the summation. Substitution of the above expression in (A.5) yields

$$\overline{\left|S_{res}\right|^2} = \overline{(a\cos\phi - 1)^2 + a^2 \sin^2\phi} \Big/ [(\Sigma A_n)^2 / (\Sigma A_n^2)] \qquad \text{(A.6)}$$

Further simplifications may be made by taking small angle approximations

$$\sin\phi \approx \phi, \ \cos\phi \approx 1$$

and substituting for the factor (a-1) the parameter (amplitude ratio error),

$$\rho = \text{amplitude error/designed value} = (a-1)A_n / A_n$$

Equation (A.6) now becomes (neglecting higher order cross product terms)

$$\overline{|S_{res}|^2} = \overline{(\rho^2 + \phi^2)} \Big/ [(\Sigma A_n)^2 / (\Sigma A_n^2)] \qquad (A.7)$$

The denominator in (A.7) is recognized as the array gain factor which will be designated g_A for either row or column.

$$g_A = (\Sigma A_n)^2 / \Sigma A_n^2 \qquad (A.8)$$

It is noted that g_A is determined by the taper sequence $|An|$, and that its value is invariant with frequency, scan angle, or element spacing as long as the taper sequence is maintained. In the determination of g_A, the elements are assumed to be isotropic.

The element gain [6], designated as g_E, is the actual element gain taken in the array in the presence of other elements and taking into account all coupling effects. An estimate of element gain of a perfectly matched array may be expressed as

$$g_E(\theta) = 4\pi A_E \cos\theta / \lambda^2 \qquad (A.9)$$

where A_E is the effective element aperture area and θ is the scan angle. At boresight, the element gain for half wavelength spacing of rows and columns is approximately 5 dB as computed from (A.9) (academically, the elements may be isotropic radiators!).

In antenna gain or pattern measurements, the operative gain (assuming a perfectly matched and lossless array) is the directive gain of the row or column, g_D, associated with the principal plane of investigation. The directive gain is the product of array and element gain factors.

$$g_D = g_A g_E \qquad \text{(A.10)}$$

It follows from equations (A.9) and (A.10) that changes in frequency, element spacing or scan angle will vary g_D proportionally to g_E.

When sidelobe residue is observed in pattern measurements, where normalization is performed with respect to directive gain, the sidelobe level is expressed, in accordance with equations (A.7), (A.8) and (A.10) as

$$\text{residue (normalized to } g_D) = \left[(\rho^2 + \phi^2)/g_D\right] g_E \qquad \text{(A.11)}$$

In the near-in sidelobe region, where g_E is nearly constant at its maximum, the mean measured residue scales down effectively from g_A as given in equation (A.7). Accordingly, the residue is invariant with changes in frequency or element spacing. However, the residue measurements track the gain roll-off of g_E and will vary accordingly with large pattern angles.

A.2 EQUIVALENCE BETWEEN ARRAY GAIN FACTOR AND 3 DB BEAMWIDTH

It is instructive to derive the equivalence between gain as given in (A.8) and the 3 dB beamwidth. The derivation that follows is based on the assumption that, relative to a uniformly illuminated array, a tapered array's beamwidth increases with taper inefficiency, i.e.,

$$(bw) \approx b_u/eff = .886\ (\lambda/Ns)/eff \qquad (A.12)$$

(bw) = 3 dB beamwidth of tapered array

b_u = 3 dB beamwidth of uniform illuminated array

eff = illumination efficiency (or taper losses)

Ns = aperture distance in wavelength (or N times the element spacing)

λ = wavelength

It is noted that the array gain factor for a uniformly illuminated array of N elements is from (A.8) equal to N. Hence the illumination efficiency may be expressed as the ratio

$$eff = [(\Sigma A_n)^2/\Sigma A_n^2]/N = g_A/N \qquad (A.13)$$

$$g_A = N(eff)$$

Substitution of g_A for N(eff) in (A.14), results in

$$(bw) = .886 \Big/ (s/\lambda) g_A \qquad (A.14)$$

It is interesting to note the beamwidth dependency on the array gain factor (element gain factor is irrelevant to the determination of beamwidth). It is recalled that g_A via the taper sequence as given in (A.8) relates to the sidelobe level. When the number of array elements stays the same, g_A tends to decrease with lower sidelobe designed levels. In order to lower the designed levels and maintain a constant beamwidth, it becomes necessary to increase the number of elements. An increase in the number of elements, having the same element spacing, leads to a proportional increase in the aperture area. Consequently, taper design changes for improved sidelobe performance are accompanied by an increase in aperture size.

APPENDIX B

DERIVATION OF PEAK SIDELOBE PROBABILITY CURVES

B.1 APPROXIMATION TO RICE'S PROBABILITY FUNCTION

Rice's probability density function in its original form [2] is

$$p(E/N) = (E/N^2) \exp [-(E^2 + P^2)/2N^2] \; I_o(EP/N^2) \qquad (B.1)$$

N	=	rms noise
E	=	envelope of signal plus noise, variable
P	=	signal amplitude
I_o	=	Bessel function of zero order, imaginary argument

The probability of E/N not to exceed a given threshold T/N (normalized) is expressed as

$$\text{prob } (E/N \leq T/N) = \int_0^{T/N} p(E/N) \, dE \qquad (B.2)$$

An approximation of (B.2) is given by North [3] as

$$\text{prob } (E/N \leq T/N) \approx (1 - \text{erf}x)/2 \qquad (B.3)$$

where

$$\text{erf}x = (2/\sqrt{\pi}) \int_0^x \exp (-y^2) dy, \qquad (B.4)$$

and

$$x = (\sqrt{1 + (P/N)^2} - T/N) / 2 \qquad (B.5)$$

Values for the error function of x, erfx, may be found in tables [5] or solved directly from (B.4). One solution of (B.4) is the following series expansion [5].

$$\text{erfx} = (2x/\sqrt{\pi}) \sum_{n=0}^{\infty} (-1)^n x^{2n}/[n!(2n+1)] \qquad \text{(B.6)}$$

In computations made in this paper, the first eight terms of the series expansion of (B.6) were included in the evaluation of erfx.

B.2 COMPUTATIONAL PROCESS IN FIGURE 3 PLOTS

In the generation of plots in figure 3, the computational process was carried out in the following manner:

1. Figure 3 plots the probability (equation B.3) for a run of the variable T/N (1 to 16 dB in steps of 0.5 dB) for parametric values of P/N ratios.

2. For each run, x computes from equation (B.5) for each pair (P/N, T/N), then erfx computes from equation (B.6) and prob ($E/N < T/N$) computes from equation (B.3).

3. A correspondence is made between signal and sidelobe parameters as follows:

N $\longleftrightarrow$ rms residual sidelobes
P $\longleftrightarrow$ sidelobe peak design value
T $\longleftrightarrow$ sidelobe specified level
E $\longleftrightarrow$ design plus random residual variable

B.3 COMPUTATIONAL PROCESS IN FIGURE 4 PLOTS

In the generation of the plot in figure 4, the following computational process was performed:

1. The probability assumes parametric values of 0.85, 0.875, 0.9, 0.925, 0.95 and respective values of erfx compute from equation (B.3).

2. From table of erfx, values of x for respective erfx are obtained.

3. For each x, T/N is set to run from 5 to 15 dB in small increments, and P/N is computed vs. T/N from equation (B.5).

4. For each pair (P/N, T/N) in item 3 above, the ratio is derived

$$T/P = (T/N)/(P/N) \qquad (B.7)$$

T/P relates to specified/design ratio.

5. Figure 4 plots T/N vs. T/P for the parametric values of the probability given in item 1 above.